

# Solid-State Studies on a C<sub>60</sub> Solvate Grown from 1,1,2-Trichloroethane

F. Michaud,<sup>†,‡</sup> M. Barrio,<sup>†</sup> D. O. López,<sup>†</sup> J. Ll. Tamarit,<sup>\*,†</sup> V. Agafonov,<sup>‡</sup>  
S. Toscani,<sup>§</sup> H. Szwarc,<sup>⊥</sup> and R. Céolin<sup>†,¶</sup>

*Departament de Física i Enginyeria Nuclear, ETSEIB, Universitat Politècnica de Catalunya, Diagonal 647, 08028 Barcelona, Catalonia, Spain, Laboratoire de Chimie Physique, Faculté de Pharmacie, 31 avenue Monge, 37200 Tours, France, Laboratoire de Chimie Physique, Faculté de Pharmacie, 4 avenue de l'Observatoire, 75006 Paris, France, and Laboratoire de Chimie Physique, UMR 8611, Université Paris Sud–CNRS, bâtiment 490, 91405 Orsay Cedex, France*

*Received June 21, 2000. Revised Manuscript Received August 31, 2000*

Single and 10-fold-twinned crystals of the C<sub>60</sub> 1:1 solvate formed with 1,1,2-trichloroethane were examined by means of scanning electron microscopy, X-ray diffraction, and differential scanning calorimetry and thermogravimetry. Solubility of C<sub>60</sub> in 1,1,2-trichloroethane was found to be 130 ± 10 mg per liter of solution in equilibrium with solvate crystals at 296 ± 2 K. The lattice metrics of the solvate is orthorhombic ( $a = 10.164(3)$  Å,  $b = 31.390(6)$  Å,  $c = 10.130(4)$  Å,  $\beta = 90.00(2)^\circ$ ), with axis  $c$  as a twin axis, although the symmetry is monoclinic (space group  $P2_1/n$ ). The solvate forms with a negative excess volume ( $-58$  Å<sup>3</sup> per formula unit), and its packing coefficient (0.76) is higher than that for close packing of hard spheres. On heating, desolvation into cubic C<sub>60</sub> and TCAN vapor occurs in one step at 436 K (onset) with a related enthalpy, +48 kJ per mole of solvate, close to the sublimation enthalpy for pure solvent. On aging at room temperature in the dark, no degradation of big ( $\approx 1 \times 10^{-3}$  mm<sup>3</sup>) solvate crystals into fcc C<sub>60</sub> is observed after 4 years have elapsed.

## 1. Introduction

Fullerene C<sub>60</sub> is known to interact with solvents of crystallization, and, after solvents have evaporated from C<sub>60</sub> solutions, it is recovered as crystalline powders made of either cubic C<sub>60</sub> crystals with noticeable amounts of strongly retained solvent<sup>1</sup> or solvate crystals, i.e., compounds with a stoichiometric ratio between C<sub>60</sub> and solvent molecules.<sup>2</sup> It was also disclosed that fullerene solvates can crystallize in the shape of decagonal crystals, reminiscent of hypothetical molecular quasi-crystalline state.<sup>3,4</sup> In addition, it was shown that C<sub>60</sub> powders can be made of mixtures of hexagonal and cubic packings;<sup>5,6</sup> hexagonal single crystals were recently

characterized,<sup>7</sup> thus indicating that polymorphism of C<sub>60</sub> is solvent-dependent, as it is for drugs.<sup>8</sup>

However, experimental results are still wanting with respect to what seems necessary to understand interactions between C<sub>60</sub> and solvent molecules in the solid state and influence of solvents on C<sub>60</sub> molecular packing.

In this paper, crystallographic, thermodynamic, and aging studies of the C<sub>60</sub>·1,1,2-trichloroethane 1:1 compound are reported, as another example of C<sub>60</sub> solvate, in the framework on C<sub>60</sub> interactions in the solid state.

## 2. Experimental Section

Cubic C<sub>60</sub> and 1,1,2-trichloroethane (TCAN) were purchased from Term USA (purity > 99.6%) and Aldrich (99%), respectively. TCAN was distilled twice before use.

Dissolution of cubic C<sub>60</sub> in TCAN at 296 ± 2 K was studied by means of absorption spectroscopy (SECOMAN S1000 spectrophotometer) at 330 and 406 nm. Optical density measurements as a function of time were performed on filtered samples pipetted from solutions stirred with an excess of solid.

Solutions of cubic C<sub>60</sub> in TCAN were allowed to evaporate in the dark at room temperature. Platelike and needle-shaped crystals were obtained, and their morphologies were examined by means of JEOL JSM35C and GEMINI BSM982 scanning electron microscopes.

Preliminary single-crystal X-ray diffraction studies were carried out with ENRAF-NONIUS and STOE Weissenberg cameras, using radiation Cu K $\alpha$  ( $\lambda = 1.5418$  Å). For the crystal symmetry to be determined, intensities were collected without

(7) Céolin, R.; Tamarit, J. Ll.; López, D. O.; Barrio, M.; Agafonov, V.; Allouchi, H.; Moussa, F.; Szwarc, H. *Chem. Phys. Lett.* **1999**, *314*, 21.

(8) Byrn, S. R. *Solid-State Chemistry of Drugs*; Academic Press: New York, 1982.

\* To whom correspondence should be addressed. Tel: 34 93 401 65 64. Fax: 34 93 401 18 39. E-mail: JOSE.LUIS.TAMARIT@UPC.ES.

<sup>†</sup> Universitat Politècnica de Catalunya.

<sup>‡</sup> Laboratoire de Chimie Physique, Faculté de Pharmacie, Tours, France.

<sup>§</sup> Laboratoire de Chimie Physique, Faculté de Pharmacie, Paris, France.

<sup>⊥</sup> Université Paris Sud–CNRS.

<sup>¶</sup> Permanent address: Laboratoire de Chimie Physique, Faculté de Pharmacie, 4, avenue de l'Observatoire, 75006 Paris, France.

(1) Fischer, J. E. *Mater. Sci. Eng. B* **1993**, *19*, 90.

(2) Céolin, R.; Michaud, F.; Toscani, S.; Agafonov, V.; Tamarit, J. Ll.; Dworkin, A.; Szwarc, H. In *Recent Advances in the Chemistry and Physics of Fullerenes and Related Materials*, Kadish, K. M.; Ruoff, R. S., Eds.; The Electrochemical Society: Pennington, NJ, 1997; Vol. 5, p 373.

(3) Fleming, R. M.; Kortan, A. R.; Hessen, B.; Siegreist, T.; Thiel, F. A.; Marsh, P.; Haddon, R. C.; Tycko, R.; Dabbagh, G.; Kaplan, M. L.; Mujsce, A. M. *Phys. Rev. B* **1991**, *44*, 888.

(4) Michaud, F.; Barrio, M.; Toscani, S.; López, D. O.; Tamarit, J. Ll.; Agafonov, V.; Szwarc, H.; Céolin, R. *Phys. Rev. B* **1998**, *57*, 10351.

(5) Vaughan, G. B. M.; Chabre, Y.; Dubois, D. *Europhys. Lett.* **1995**, *31*, 525.

(6) Archangel'skii, I. V.; Skokan, E. V.; Velikodnyi, Yu. A.; Chernyshev, V. V.; Sidorov, L. N. *Dokl. Phys. Chem.* **1998**, *363*, 413.

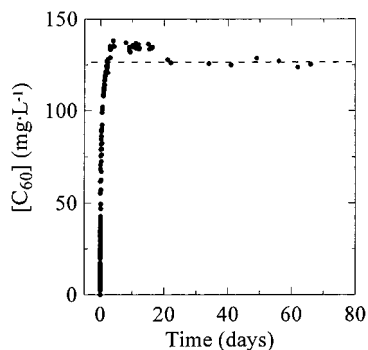


**Figure 1.** Dissolution curve of  $C_{60}$  in 1,1,2-trichloroethane (TCAN) at room temperature (296 K).

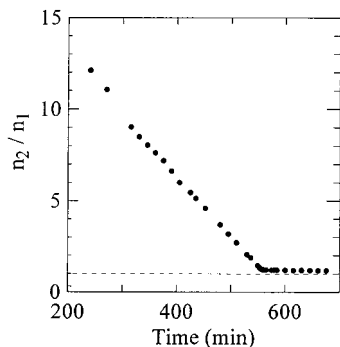


**Figure 2.** Evaporation curve of a diluted solution of  $C_{60}$  in 1,1,2-trichloroethane (TCAN) at room temperature (299 K). Numbers  $n_1$  and  $n_2$  stand for the  $C_{60}$  and TCAN moles in the medium, respectively.

constraint over one hemisphere by means of an ENRAF-NONIUS CAD-4 four-circle diffractometer.

X-ray powder diffraction profiles were recorded by means of INEL CPS120 diffractometers (Debye-Scherrer geometry, transmission mode, Cu  $K\alpha_1$  radiation ( $\lambda = 1.5406 \text{ \AA}$ )).

Thermogravimetry (TG) and differential scanning calorimetry (DSC) were performed under nitrogen flux at a  $10 \text{ K}\cdot\text{min}^{-1}$  rate using the thermobalance and the DSC cell of a TA INSTRUMENTS TA2000 apparatus, respectively. Low-temperature DSC experiments (100–300 K range) were carried out at 10 or  $2 \text{ K}\cdot\text{min}^{-1}$  rates with a PERKIN-ELMER DSC7 apparatus equipped with a homemade cooling device. The uncertainty in the measured enthalpy changes is considered to be lower than 5%. Sample masses were weighed by means of 0.01 mg sensitive balances.

### 3. Results

**3.1. Dissolution, Solubility, and Stoichiometry Studies.** Three steps in the dissolution curve can be observed in Figure 1. First, cubic  $C_{60}$  dissolves in TCAN, and the slope of the dissolution curve is found to be about  $780 \text{ mg of } C_{60} \text{ per solvent liter and per day}$  at time  $t = 0$ . Then, dissolution goes through a maximum before leveling at a constant value in the third step. This value, which corresponds to the solubility of  $C_{60}$  in TCAN at  $296 \pm 2 \text{ K}$ , was found to be  $130 \pm 10 \text{ mg of } C_{60} \text{ per liter of saturated solution}$ . However, solutions with  $C_{60}$  concentrations as high as  $222 \text{ mg of } C_{60} \text{ per liter of solution}$  were prepared at room temperature by dissolving cubic  $C_{60}$  by means of ultrasound without any subsequent precipitation.

A diluted solution, made of initially known masses of  $C_{60}$  and TCAN, was allowed to evaporate at 299 K, and the solution weight was measured as a function of time (Figure 2). It reached a minimum indicating that the

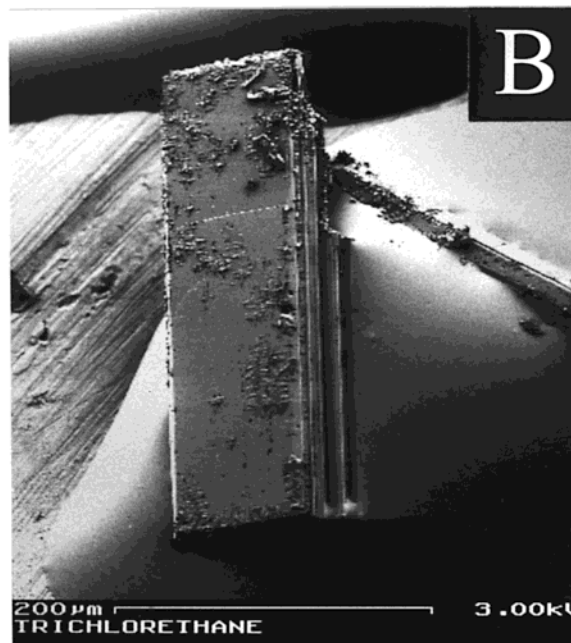


**Figure 3.** Scanning electron microscopy (SEM) photographs of  $C_{60}\cdot 1$  TCAN crystals. (A) Cross of two decagonal needles glued on the sample holder in the same vertical position as that in the crystallization beaker (accelerating voltage = 15 kV, white bar =  $100 \mu\text{m}$ ). (B) Platelike single crystal (accelerating voltage = 3 kV, white bar =  $200 \mu\text{m}$ ).

crystals formed after TCAN excess had evaporated are solvate crystals with 1:1 molar ratio between TCAN and  $C_{60}$ .

**3.2. Crystallographic Studies.** Two kinds of crystals were examined: 10-sided prisms of about  $0.05\text{--}0.10 \text{ mm}$  thickness and up to  $1 \text{ mm}$  length (Figure 3A), and rectangular plates with dimensions of about  $0.2\text{--}0.3 \times 0.05\text{--}0.1 \times 0.005\text{--}0.01 \text{ mm}^3$  (Figure 3B).

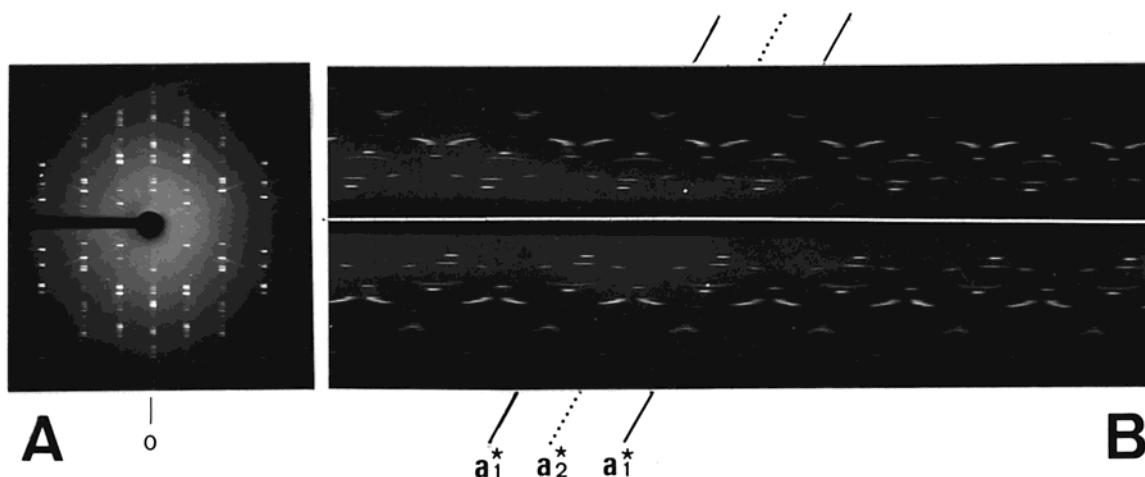


**Figure 4.** Oscillation (A) and zero-layer Weissenberg (B) photographs of a decagonal needle-shaped crystal of C<sub>60</sub>·1 TCAN solvate rotating about the needle axis. Photograph A shows that the oscillation axis is a symmetry axis. Photograph B shows that angles between axes  $a_1'$  and  $a_2'$  and between two consecutive  $a'$  axes are 18° and 36°, respectively.

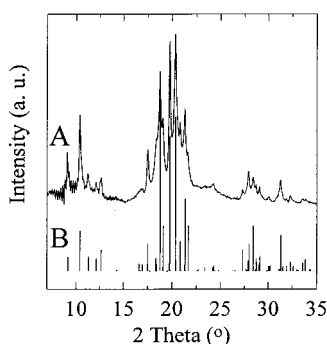


**Figure 5.** X-ray powder profile of the C<sub>60</sub>·1 TCAN solvate. (A) Experimental profile obtained from unground crystals in an excess of mother liquor; (B) profile calculated with intensities collected from a single crystal and taking multiplicity factors into account.

X-ray diffraction photographs (Figure 4A) of needles oscillating about their growth axis revealed the apparent  $m$  symmetry. The oscillation axis parameter was found to be  $c' = 10.11$  Å. Zero-layer Weissenberg photographs (Figure 4B) showed features similar to those obtained with other C<sub>60</sub> solvates,<sup>3,4</sup> indicating that needle-growth axis  $c'$  is a 10-fold axis. These features were related to the 10-time repeat through a 36° rotation around axis  $c'$  of a lattice whose axes  $a' = 10.17$  Å and  $b' = 31.18$  Å were tentatively assigned to an orthorhombic unit cell by analogy with previous findings.<sup>4,9,10</sup>

The same orthorhombic metrics was found from single crystals, using oscillation and Weissenberg techniques as well as automatic search procedures of the four-circle diffractometer. Least-squares refinement (25 reflections) of the unit-cell parameters yielded  $a' = 10.164(3)$  Å,  $b' = 31.390(6)$  Å,  $c' = 10.130(5)$  Å,  $\alpha = 90.03(3)^\circ$ ,  $\beta = 89.98(3)^\circ$ , and  $\gamma = 90.08(3)^\circ$ .

The X-ray powder profile (Figure 5A) of small unground crystals surrounded with mother liquor inside

**Table 1.** X-ray Powder Diffraction Data for Solvate C<sub>60</sub>·1 TCAN at 298 K (Observed and Calculated  $2\theta$  Values Correspond to the Profile in Figure 5A) and Comparison with Single-Crystal Data Obtained for the Same Solvate<sup>a</sup>

single crystal					powder				
h	k	l	$2\theta$	$II_0$	no.	$2\theta_{\text{obsvd}}$	$2\theta_{\text{calcd}}$	$2\Delta\theta$	$II_0$
1	1	0	9.138	8	1	9.100	9.150	0.050	12
0	2	1	10.385	22	2*	10.390	10.382	0.008	37
0	4	0	11.266	8	3*	11.259	11.250	0.009	7
1	3	0	12.130	7	4*	12.106	12.132	0.026	4
1	1	1	12.645	8	5*	12.650	12.650	0.000	8
1	5	0	16.584	4			16.574		-
0	6	0	16.934	4			16.908		-
2	0	0	17.436	4			17.464		-
0	0	2	17.495	15	6*	17.496	17.500	0.004	16
2	2	0	18.335	7	7*	18.362	18.358	0.004	30
0	2	2	18.391	7			18.392		-
1	5	1	18.766	100	8*	18.784	18.754	0.030	66
0	6	1	19.077	25	9*	19.084	19.056	0.028	27
1	1	2	19.771	73	10*	19.775	19.772	0.003	75
2	2	1	20.336	75	11*	20.345	20.350	0.005	100
2	4	0	20.807	15			20.822		-
0	4	2	20.857	16	12*	20.855	20.852	0.003	41
1	3	2	21.344	39	13*	21.334	21.340	0.006	43
1	7	0	21.643	25	14*	21.634	21.622	0.012	9
2	4	2	27.312	12	15	27.380	27.314	0.066	5
3	1	1	27.890	6			27.921		-
1	7	2	27.964	5	16*	27.925	27.944	0.019	17
1	1	3	27.966	14			27.967		-
1	9	1	28.431	24	17*	28.380	28.398	0.018	13
2	8	0	28.721	7	18*	28.696	28.710	0.014	7
0	8	2	28.758	5			28.734		-
3	3	1	29.048	4	19*	29.091	29.076	0.015	6
1	3	3	29.121	8			29.118		-
3	5	1	31.247	10	20*	31.261	31.266	0.005	9
1	5	3	31.315	20			31.366		-

<sup>a</sup> Symbol \* indicates reflections used for least-squares refinement.  $II_0$  (%) = relative intensities.

a Lindemann capillary tube (0.5 mm diameter) was found to be in fair agreement with the profile calculated (Figure 5B and Table 1) using intensity vs  $2\theta$  values measured with the four-circle diffractometer.

However, systematic extinctions did not fit with any orthorhombic space group. This was confirmed by measuring without constraints the intensities of the reflections over one hemisphere and observing conditions limiting reflections for monoclinic space group  $P2_1/n$  (no. 14), cell choice 2 ( $hkl$ , no condition;  $h0$ ,  $h + l = 2n$ ;  $0k0$ ,  $k = 2n$ ).<sup>11</sup>

(9) Céolin, R.; Agafonov, V.; Moret, R.; Fabre, C.; Rassat, A.; Dworkin, A.; André, D.; Szwarc, H.; Schierbeek, A. J.; Bernier, P.; Zahab, A. *Carbon* **1992**, *30*, 1121.

(10) Agafonov, V.; Céolin, R.; Moret, R.; André, D.; Dworkin, A.; Szwarc, H.; Fabre, C.; Rassat, A.; Cense, J. M.; Zahab, A.; Bernier, P. *J. Cryst. Growth* **1992**, *123*, 366.

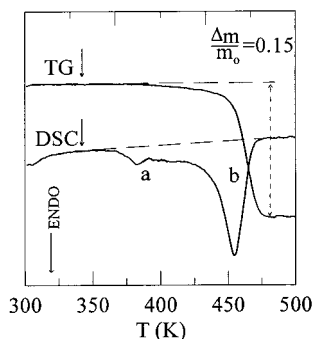


**Figure 6.** TG and DSC curves recorded on heating  $C_{60}$ -1 TCAN crystals gathered in punctured pans ( $N_2$  flow,  $10\text{ K}\cdot\text{min}^{-1}$  rate). Sample masses:  $0.92\text{ mg}$  (TG),  $1.81\text{ mg}$  (DSC).

Then, the parameters of the monoclinic unit cell were least-squares refined using the  $2\theta$  values of 30 reflections (Table 1) collected with the single-crystal diffractometer. They were found to be  $a = 10.164(3)\text{ \AA}$ ,  $b = 31.390(6)\text{ \AA}$ ,  $c = 10.130(4)\text{ \AA}$ ,  $\beta = 90.00(2)^\circ$ .

As a control, they were also refined using  $2\theta$  values of 18 peaks of the X-ray powder profile (Table 1). The results were  $a = 10.148(8)\text{ \AA}$ ,  $b = 31.437(20)\text{ \AA}$ ,  $c = 10.128(9)\text{ \AA}$ ,  $\beta = 89.94(6)^\circ$ , close to those reported above.

**3.3. Thermodynamic Studies.** Because it was observed that mechanical treatment entails desolvation<sup>12</sup> or amorphization,<sup>13</sup> crystals were gently picked up one after another from the beakers and gathered into pierced aluminum pans for TG and DSC experiments in order to analyze the thermal behavior of the  $C_{60}$ -1 TCAN solvate.

The TG curve in Figure 6 shows that a 15% weight loss occurred almost in one step at about  $440\text{ K}$  (onset). This is close to the value (15.6%) calculated assuming a 1:1 molar ratio between  $C_{60}$  and TCAN in the solvate lattice, and it goes along with the result shown in Figure 2. It is worth noting that the  $C_{60}$  powder recovered after the TG experiment did not exhibit the sc-fcc transition near  $260\text{ K}$ .<sup>14</sup>

No thermal effect was observed in the  $298\text{--}100\text{ K}$  range when cooling the first solvate-containing DSC pans. Two endothermic peaks were recorded on heating (Figure 6) with onset temperatures of  $372\text{ K}$  (a) and  $436\text{ K}$  (b), respectively. The well-defined peak "a" (about  $+5\text{ kJ}\cdot\text{mol}^{-1}$ ) was assigned to a possible phase transition because it was not associated with any weight loss. By integrating peak "b" the desolvation enthalpy was found to be about  $+48\text{ kJ}$  per mole of solvent.

To check whether other solvates form, the  $C_{60}$ -TCAN phase diagram was studied following a method used previously.<sup>15</sup> Results are reported in Figure 7A. Melting of pure TCAN was found onsetting at  $237.8\text{ K}$  with  $\Delta_{\text{fus}}H = +10.8\text{ kJ}\cdot\text{mol}^{-1}$ , i.e., the same values as those found in the literature.<sup>16</sup> The sc-fcc  $C_{60}$  transition was found onsetting at  $259.4\text{ K}$ , instead of  $262.1\text{ K}$ , with  $\Delta_{\text{trans}}H =$

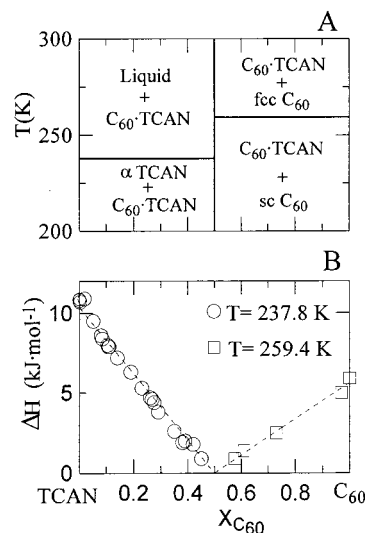


**Figure 7.**  $C_{60}$ -TCAN phase diagram: (A) phase regions ( $\alpha$ TCAN = phase  $\alpha$  of TCAN); B = Tammann curves associated with the invariant equilibria.

$+5.9\text{ kJ}\cdot\text{mol}^{-1}$  instead of  $+10.4\text{ kJ}\cdot\text{mol}^{-1}$ .<sup>14</sup> A degenerated eutectic equilibrium and a eutectoid one were observed in the TCAN-rich and in the  $C_{60}$ -rich parts of the diagram, respectively. The enthalpies associated with these equilibria were found to be 0 at  $x_{C_{60}} = 0.5$  (see Tammann curves in Figure 7B). This indicated that only the 1:1 solvate had formed.

**3.4. Aging Studies.** Three closed beakers containing solvate crystals have been kept for 4 years in the dark at room temperature. Visual observations by means of an optical microscope ( $G \times 140$ ) revealed that such crystals exhibit two ranges of sizes: SEM photograph in Figure 8A shows first-range 10-fold-twinned crystals ( $\approx 100\text{ }\mu\text{m}$  diameter). The SEM photograph in Figure 8B reveals smaller 10-fold-twinned crystals ( $\approx 10\text{ }\mu\text{m}$ ). After 4-year storage, crystals from each beaker were examined through X-ray, DSC, and/or TG measurements.

With big ( $10^6\text{ }\mu\text{m}^3$ ) crystals, X-ray profile (Figure 9A) corresponding to unground samples matches that of solvate without observable fcc  $C_{60}$ . DSC and/or TG measurements reveal enthalpies of about  $50\text{ J}$  per gram of sample and weight losses of 13–15%, respectively, which agree fairly well with expected values for the solvate.

For small ( $10^3\text{ }\mu\text{m}^3$ ) crystal samples, X-ray studies (Figure 9B) reveal mainly fcc  $C_{60}$  profiles with some solvate peaks. TG shows 4.4% weight loss, and the related enthalpy is about  $25\text{ J}$  per gram of sample at most.

Mixtures of both sizes (SEM photograph in Figure 8C, where big plates can also be seen) lead to intermediate results (enthalpies of about  $30\text{ J}$  per gram of sample, 8–12% weight losses, and X-ray profile in Figure 9C).

## 4. Discussion

The dissolution curve in Figure 1 may be understood in terms of a transition from a metastable solid-liquid equilibrium to a stable solid-liquid one: the  $C_{60}$  content

(11) *International Tables for Crystallography*, 3rd revised ed.; Hahn, T., Ed.; Kluwer Academic Publishers: Dordrecht, 1992; Vol. A, Space-Group Symmetry.

(12) Oszlányi, G.; Bortel, G.; Faigel, G.; Pekker, S.; Tegze, M. *Phys. Rev. B* **1993**, *48*, 7682.

(13) Allouchi, H.; López, D. O.; Gardette, M.-F.; Tamarit, J. Ll.; Agafonov, V.; Szwarc, H.; Céolin, R. *Chem. Phys. Lett.* **2000**, *317*, 40.

(14) Miyazaki, Y.; Sorai, M.; Lin, R.; Dworkin, A.; Szwarc, H.; Godard, J. *Chem. Phys. Lett.* **1999**, *305*, 293.

(15) Barrio, M.; López, D. O.; Tamarit, J. Ll.; Szwarc, H.; Toscani, S.; Céolin, R. *Chem. Phys. Lett.* **1996**, *260*, 78.

(16) Golovanova, Yu. G.; Kolesov, V. P. *Vestn. Mosk. Univ., Ser. 2: Khim.* **1984**, *25*, 244.

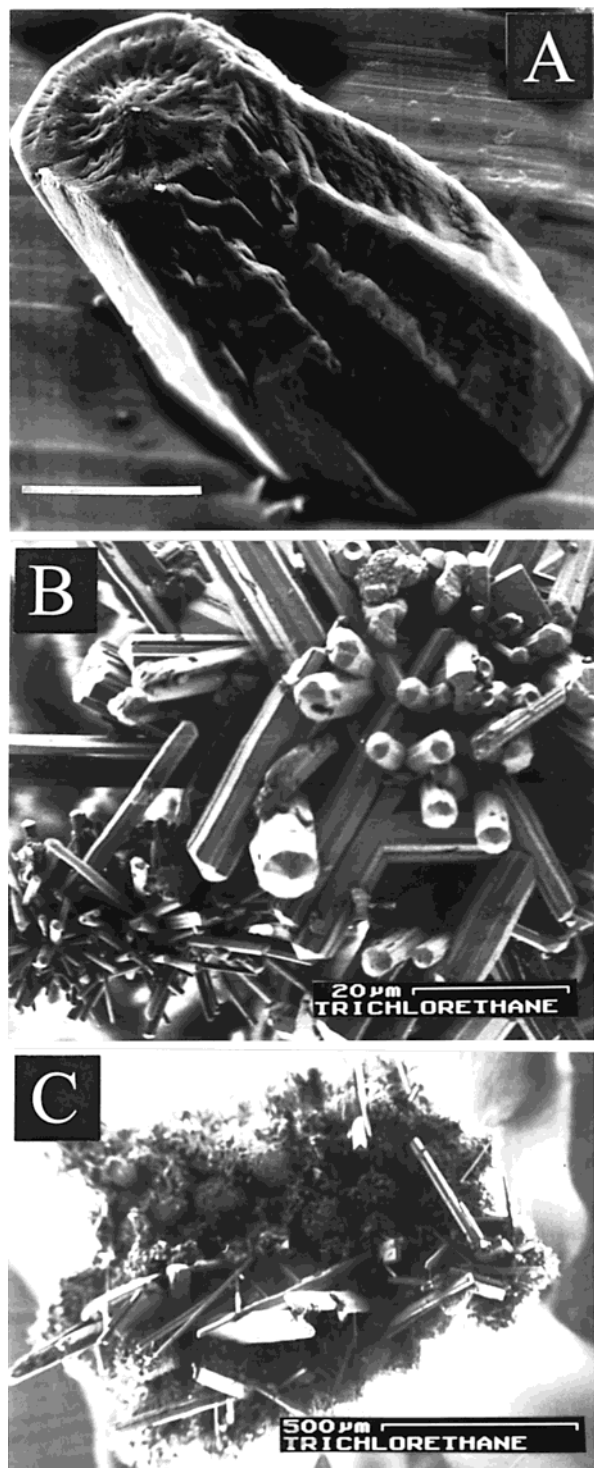


**Figure 8.** SEM photographs of crystals typical for the beakers stored for aging studies. (A) "Big" crystals from beaker A (white bar = 50  $\mu\text{m}$ , accelerating voltage (a.v.) = 15 kV); (B) "small" crystals from beaker B (white bar = 20  $\mu\text{m}$ , a.v. = 1 kV); (C) mixture of small and big crystals from beaker C (white bar = 500  $\mu\text{m}$ , a.v. = 1 kV).

in the liquid phase first increases, tending to reach the value for the saturated solution in (metastable) equilibrium with cubic C<sub>60</sub>, while solvate crystals with lower solubility begin crystallizing. This process ends when all the solid in equilibrium with the solution has transformed into the solvate. Thus the solubility, which was then measured, corresponds to the more stable equilibrium state, which was attained within no less

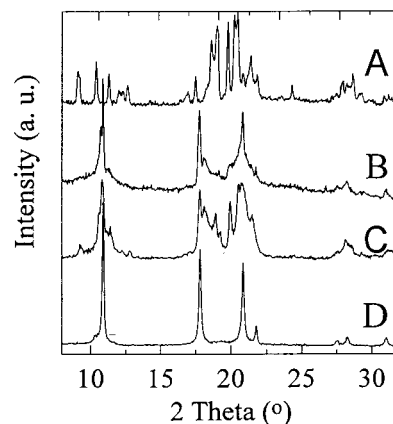


**Figure 9.** X-ray powder diffraction profiles of 4-year old samples from beakers A, B, and C. D = Typical X-ray powder diffraction profile obtained after samples were heated to 600 K.

than about 25 days at room temperature. It is to be noticed that the 130  $\text{mg}\cdot\text{L}^{-1}$  solubility in 1,1,2-trichloroethane is analogous to what is found in similar solvents (160 and 150  $\text{mg}\cdot\text{L}^{-1}$  in chloroform<sup>17</sup> and in 1,1,1-trichloroethane,<sup>18</sup> respectively).

The C<sub>60</sub> solubility was reported to be anomalous<sup>19</sup> because it goes through a maximum as temperature increases. This result is to be related to structural and composition changes that occur within the solid in excess. At lower temperatures, the metastable C<sub>60</sub>-liquid equilibrium may occur first and concentration increases as usual. Then, at higher temperatures, the solid phase coexisting with the saturated solution may transform more and more quickly into the less-soluble phase, that is, the more stable one, and this process may look like an apparent solubility decrease.

The unit-cell volume for the C<sub>60</sub>-TCAN 1:1 solvate is found to be 3232  $\text{\AA}^3$ . Assuming that there are 4 formula units per unit cell and that the molecular volume of a C<sub>60</sub> molecule is 710  $\text{\AA}^3$ , as it is in its fcc phase ( $a = 14.16 \text{ \AA}$ ), it is obtained 98  $\text{\AA}^3$  per TCAN molecule. This is close to the van der Waals molecular volume (91  $\text{\AA}^3$ ) calculated using Kitaigorodskii values, 54 and 37  $\text{\AA}^3$ , for  $-\text{HCCl}_2$  and  $-\text{H}_2\text{CCl}$  groups,<sup>20</sup> respectively. Also assuming a van der Waals volume of 526  $\text{\AA}^3$  per C<sub>60</sub> sphere with a 5  $\text{\AA}$  van der Waals radius, the packing coefficient (0.76) for the C<sub>60</sub>-TCAN solvate is higher than that for close packing of spheres (0.74), as already observed in other cases.<sup>2,4,21</sup> Because no crystal structure of TCAN was determined, an X-ray diffraction profile of solid TCAN was recorded at 223 K. It was tentatively indexed in the monoclinic system using the program DICVOL<sup>22</sup> with no unindexed reflection (Table 2). Least-squares refined unit-cell parameters were found to be  $a = 6.919(5) \text{ \AA}$ ,  $b = 10.000(7) \text{ \AA}$ ,  $c = 4.593(3) \text{ \AA}$ ,  $\beta = 100.52(4)^\circ$ ,  $V = 312.4(2) \text{ \AA}^3$ . Assuming  $Z = 2$  in the unit cell, this corresponds to 156  $\text{\AA}^3$  per TCAN molecule.

(17) Ruoff, R. S.; Malhotra, R.; Huestis, D. L.; Tse, D. S.; Lorents, D. C. *Nature* **1993**, *362*, 140.

(18) Beck, M. T.; Mándi, G. *Fullerene Sci. Technol.* **1997**, *5*, 291.

(19) Ruoff, R. S.; Tse, D. S.; Malhotra, R.; Lorents, D. C. *J. Phys. Chem.* **1993**, *97*, 3379.

(20) Kitaigorodsky, A. I. *Molecular Crystals and Molecules*; Academic Press: New York, 1973.

(21) Michaud, F.; Barrio, M.; Toscani, S.; Agafonov, V.; Szwarc, H.; Céolin, R. *Fullerene Sci. Technol.* **1997**, *5*, 1645.

(22) Louër, D.; Boulitf, A. *DICVOL91 program*; Laboratoire de Cristallogimie, Université de Rennes I: Rennes, France, 1991.

**Table 2. X-ray Powder Diffraction Data for 1,1,2-Trichloroethane at 223 K**

h	k	l	$I/I_0$	$d_{\text{obsvd}}$	$d_{\text{calcd}}$	$d_{\text{obsvd}} - d_{\text{calcd}}$
1	1	1	78	3.2919	3.2874	0.0045
1	2	1	64	3.1799	3.1820	0.0021
2	0	1	76	2.9904	2.9919	0.0015
2	1	1	100	2.8712	2.8664	0.0048
1	3	1	44	2.5929	2.5927	0.0002
2	0	1	25	2.5095	2.5059	0.0036
2	3	0	65	2.3777	2.3808	0.0031
2	1	1	93	2.4270	2.4308	0.0038
2	2	1	92	2.2404	2.2403	0.0001
0	2	2	34	2.0563	2.0577	0.0014
0	3	2	59	1.8694	1.8694	0.0000
3	1	1	71	1.8601	1.8596	0.0005
3	3	1	22	1.8314	1.8323	0.0009
1	5	1	18	1.8010	1.7997	0.0013

The  $C_{60}$ ·1 TCAN solvate forms with a negative excess volume of  $(3232/4) - (710 + 156) = -58 \text{ \AA}^3$  per formula unit, close to the value for the  $C_{60}$ ·2CCl<sub>4</sub> solvate,<sup>23</sup> and this goes along with the assumption that  $C_{60}$  and TCAN strongly interact and form 1:1 solvate.

Nevertheless, the desolvation enthalpy (+48 kJ·mol<sup>-1</sup>) is close to the sublimation enthalpy of pure TCAN (about +46 kJ·mol<sup>-1</sup>), calculated by adding the enthalpies of vaporization<sup>24</sup> (+34.8 kJ·mol<sup>-1</sup>) and of fusion<sup>16</sup> (+10.88 kJ·mol<sup>-1</sup>). This indicates that interactions between  $C_{60}$  and TCAN in the solvate network are weak interactions. Such a paradoxical outcome, which has already been reported,<sup>2</sup> remains to be explained.

The  $C_{60}$ -TCAN 1:1 solvate is another example of  $C_{60}$  solvate exhibiting 10-fold twinning. Until now, all  $C_{60}$  solvates, for which both single and decagonal crystals were examined, exhibit orthorhombic lattices with similar parameters.<sup>4,21</sup> As pointed out previously,<sup>3</sup> the two-dimensional point lattice, perpendicular to the 10-fold axis, may be related to a monoclinic metrics with reciprocal angle  $\beta^*$  close to  $72^\circ$  (i.e.,  $360^\circ/5$ ). For solvate  $C_{60}$ ·1 TCAN, this corresponds to a metrics with parameters  $a_M = a = 10.164 \text{ \AA}$ ,  $b_M = c = 10.130 \text{ \AA}$ ,  $c_M = (a + b)/2 = 16.497 \text{ \AA}$ ,  $\beta_M = 180.00^\circ - 72.06^\circ = 107.94^\circ$ . So the  $c_M/a_M$  ratio (1.623) is close to the golden ratio ( $\tau = 1.618\ 033\dots$ ). In the case of the  $C_{60}$ ·DCAN 1:1 solvate (DCAN = 1,2-dichloroethane), the pericline law of twinning,<sup>4</sup> with  $72^\circ$  between two adjacent two-variant twins (and a  $35.63^\circ$  angle between the two variants in each twin), has been shown to account for decagonal twinning with an irrational  $(-1\ K0)$  composition plane between the individuals of each two-variant twin. For  $C_{60}$ ·1 TCAN, the  $K$  value ( $K = (b/a)^2 = 9.538\dots$ ) and the angle between two adjacent faces ( $2 \arctan(a/b) = 35.88^\circ$ ) are close to 9.696... and  $35.63^\circ$  for the  $C_{60}$ ·1 DCAN solvate, respectively. However, some decagonal crystals of the  $C_{60}$ ·1 TCAN solvate were found with dihedral angles between adjacent lateral faces to be quite different from  $36^\circ$ . For instance, a series of 34, 26, 24, 41, 40, 39.5, 38, 38, 35.5, and  $44^\circ$  angles were measured with an uncertainty of about  $\pm 1^\circ$  between adjacent lateral faces of the crystal whose diffraction

patterns are shown in Figure 4. This indicates that, contrary to preceding observations,<sup>4</sup> growth of  $C_{60}$  decagonal twins does not need lateral faces to be in the same form. For instance, the dihedral angles between face  $\{1\ 0\ 0\}$  and faces  $\{1\ 2\ 0\}$ ,  $\{1\ 3\ 0\}$ ,  $\{2\ 3\ 0\}$ ,  $\{3\ 8\ 0\}$  are 32.92, 44.17, 25.91, 40.81°, respectively, while the angle between  $\{1\ 1\ 0\}$  and  $\{1\ -1\ 0\}$  is  $35.98^\circ$ . Moreover, it was conjectured<sup>4</sup> that such twins grow from either a one-dimensional icosahedral nucleus or an initial composition plane, thus leading to 10-sided needles (see Figure 3A) or to a spiral growth,<sup>10</sup> respectively. Among crystals of  $C_{60}$ ·1 TCAN, 10-sided rods with and without central empty channels were found, and, surprisingly, very thin needles such as that shown in Figure 10A were also observed. This might go along with the first hypothesis, which may be illustrated in Figure 10: the section in Figure 10C shows that needles are near cylinders with diameters as small as about  $7\ \mu\text{m}$ , which correspond to about 7000  $C_{60}$  molecules. Unfortunately, such needles with almost circular sections were too thin for X-ray diffraction to be performed.

This work also shows that orthorhombic symmetry is not required for decagonal twinning to occur. However, the  $C_{60}$ ·1 TCAN lattice symmetry departs only weakly from orthorhombic symmetry. In the  $P2_1/n$  setting chosen to describe this lattice, condition  $0\ k\ l$ :  $k = 2n$ , which would turn the actual space group into orthorhombic space group  $Pbnm$ , is removed by only few weak reflections with  $I > 2\sigma(I)$ : e.g.,  $0\ 1\ 1$ ,  $0\ 3\ 1$ ,  $0\ 3\ 2$ ,  $0\ 3\ 3$ ,  $0\ 7\ 3$ ,  $0\ 1\ 5$ , whose intensities were averaged over  $I(0\ k\ l)$  and  $I(0\ k\ -l)$ . It resulted  $I(\sigma(I)) = 61(4)$ ,  $31(3.5)$ ,  $7.5(2.3)$ ,  $11.5(2.1)$ ,  $4.8(1.7)$ , and  $20.3(1.6)$ , respectively (to be compared with the highest  $I$  value  $I(\sigma(I)) = 3200(30)$  for reflection  $1\ 5\ 1$ ). So it can be said that, within experimental accuracy, symmetry departs very weakly from orthorhombic.

Also taking into account that the X-ray powder profile of  $C_{60}$ ·1 TCAN is almost the same as those of the orthorhombic  $C_{60}$  solvates formed with DCAN<sup>4</sup> and  $n$ -pentane,<sup>25</sup> it may be inferred that packing of  $C_{60}$  molecules in the  $C_{60}$ ·1 TCAN lattice is akin to a model proposed previously.<sup>26,27</sup> However, TCAN molecular symmetry (no mirror plane normal to the C-C bond) and possible orientational disorder of TCAN (e.g., rotation or large amplitude libration about the C-C bond) may account for the lowered symmetry in  $C_{60}$ ·1 TCAN crystals with respect to the orthorhombic solvates. Anyway, an orthorhombic-to-monoclinic transition was previously observed when cooling the  $C_{60}$ ·1  $n$ -pentane solvate<sup>28</sup> whose lattice remains C-centered. Removing the  $m$  symmetry in the solvent molecule might thus remove the C-centering. Orthorhombic symmetry would be recovered at high temperature in the  $C_{60}$ -TCAN solvate, just before starting to lose solvent, when thermal expansion gives space enough for isotropic orientational disorder to occur in the TCAN sites, as suggested by the endothermic DSC peak at 372 K (Figure 6). After heating the sample up to 400 K, room-

(23) Céolin, R.; Agafonov, V.; André, D.; Dworkin, A.; Szwarc, H.; Dugué, J.; Keita, B.; Nadjjo, L.; Fabre, C.; Rassat, A. *Chem. Phys. Lett.* **1993**, *208*, 259.

(24) Majer, V.; Svoboda, V. *Enthalpies of Vaporization of Organic Compounds: A Critical Review and a Data Compilation*; Blackwell Scientific Publications: Oxford, 1985.

(25) Pekker, S.; Faigel, G.; Fodor-Csorba, K.; Gránásky, L.; Jakab, E.; Tegze, M. *Solid State Commun.* **1992**, *83*, 423.

(26) Morosin, B.; Xiang, X. D.; Zettl, A. (unpublished). Reference note in: Assink, R. A.; Schirber, J. E.; Loy, D. A.; Morosin, B.; Carlson, G. A. *J. Mater. Res.* **1992**, *7*, 2136.

(27) Oszlányi, G.; Bortel, G.; Faigel, G.; Pekker, S.; Tegze, M. *Solid State Commun.* **1994**, *98*, 417.

(28) Faigel, G.; Bortel, G.; Oszlányi, G.; Pekker, S.; Tegze, M.; Stephens, P. W.; Liu, D. *Phys. Rev. B* **1994**, *49*, 9186.

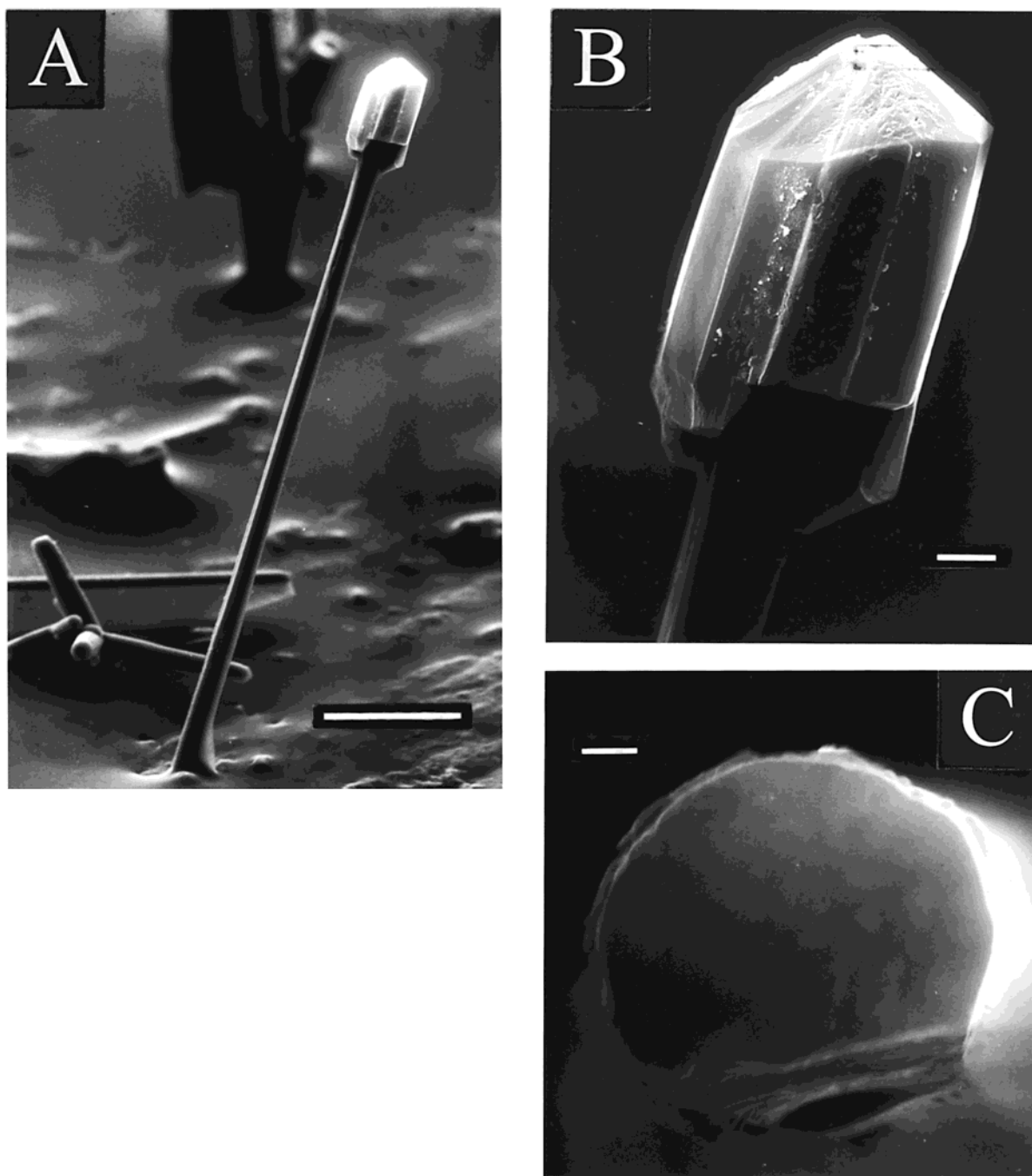


**Figure 10.** Scanning electron microscopy photograph (accelerating voltage = 25 kV) of a 10-sided crystal at the top of a needle glued on the sample holder in the same near-vertical position as that observed in the crystallization beaker. (A) General view (white bar = 100  $\mu\text{m}$ ); (B) detail of the top of the needle (white bar = 10  $\mu\text{m}$ ); (C) nearly circular section of a needle similar to that in (A) (white bar = 1  $\mu\text{m}$ ).

temperature X-ray measurements reveal the same profile as that of unheated samples. This supports the phase transition hypothesis. Thus, the 372 K peak is not to be assigned to some lattice destruction process.

Whether solvates persist as such in air or decompose into a disordered fcc C<sub>60</sub> lattice is still an open question.<sup>29</sup> Solvent-rich solvates, such as the C<sub>60</sub>·*n* cyclohexane solvate,<sup>30</sup> lose their crystallization solvent as

soon as they are removed from their mother liquor, while solvates with lower solvent content, such as C<sub>60</sub>·2CCl<sub>4</sub>,<sup>23</sup> seem to be air stable for 1 year at least. However, the C<sub>60</sub>·1 DCAN solvate was shown to degrade spontaneously within a few days,<sup>4</sup> and, in this case, adsorption of solvent on cubic C<sub>60</sub> was shown to be

(31) Céolin, R.; Agafonov, V.; Toscani, S.; Gardette, M.-F.; Gonthier-Vassal, A.; Szwarc, H. *Fullerene Sci. Technol.* **1997**, *5* (3), 559.

(32) Céolin, R.; Agafonov, V.; Bachet, B.; Gonthier-Vassal, A.; Szwarc, H.; Toscani, S.; Keller, G.; Fabre, C.; Rassat, A. *Chem. Phys. Lett.* **1995**, *244*, 100.

(33) Gardette, M.-F.; Chilouet, A.; Toscani, S.; Allouchi, H.; Agafonov, V.; Rouland, J.-C.; Szwarc, H.; Céolin, R. *Chem. Phys. Lett.* **1999**, *306*, 149.

(29) Collins, C.; Foulkes, J.; Bond, A. D.; Klinowski, J. *Phys. Chem. Chem. Phys.* **1999**, *1*, 5323.

(30) Gorun, S. M.; Creegan, K. M.; Sherwood, R. D.; Cox, D. M.; Day, V. W.; Upton, R. M.; Briant, C. E. *J. Chem. Soc., Chem. Commun.* **1991**, 1556.

preferred to solvate formation by about  $-10$  kJ per mole of solvent.

According to measurements performed after 4-year aging, solvate  $C_{60}\cdot 1$  TCAN spontaneously decomposes into cubic  $C_{60}$  at room temperature. However, this transformation proceeds very slowly as big crystals remain unchanged according to high-resolution X-ray powder diffraction.

Furthermore, X-ray diffraction profiles such as that in Figure 9D were recorded at room temperature after 4-year old batches were heated to about 600 K. This profile, which is that for pure fcc  $C_{60}$  with disorder and stacking faults,<sup>5</sup> seems to indicate that, on aging,  $C_{60}$  molecules neither degraded in air nor reacted with solvent molecules.

### 5. Concluding Remarks

Although  $C_{60}\cdot 1$  TCAN solvate forms with a negative excess volume and a very dense packing, solvent molecules leave crystals on heating as if they were almost free from interactions with  $C_{60}$  molecules. As data pile up along (Table 3), this appears to be a common feature of fullerene solvates and becomes all the more paradoxical as solvent removal from cubic  $C_{60}$  powders is very difficult.<sup>1</sup>

Because solvent is lost in one step on heating  $C_{60}\cdot 1$  TCAN crystals, the solvation vs adsorption thermodynamic balance cannot be determined for the  $C_{60}$ -TCAN system as it was for the  $C_{60}$ -DCAN one.<sup>4</sup> However, it may be inferred, from aging studies reported here, that trapping of solvent molecules by fcc  $C_{60}$  powders mainly occurs through solvation when TCAN is used as a crystallization solvent.

**Table 3. Excess Volume Per Formula Unit ( $V_E$ ), Desolvation Enthalpy ( $\Delta H_D$ ), and Sublimation Enthalpy ( $\Delta H_S$ ) per Mole of Solvent for Some  $C_{60}$  Solvates**

solvate	$V_E / \text{\AA}^3$	$\Delta H_D / \text{kJ}\cdot\text{mol}^{-1}$	$\Delta H_S / \text{kJ}\cdot\text{mol}^{-1}$	ref
$C_{60}\cdot 1$ <i>n</i> -octane	$\approx -24$	50	55	31
$C_{60}\cdot 1$ <i>n</i> -heptane	$\approx -20$	35.5	37.3	32
$C_{60}\cdot 1$ $\text{Cl}_2\text{C}=\text{CHCl}$	$\approx -40$	43.7	40.6	21
$C_{60}\cdot 2$ $\text{CCl}_4$	$\approx -50$	37	34.2	23
$C_{60}\cdot 2$ $\text{S}_8$	$\approx -42$ or $\approx -63$	93	97	33
$C_{60}\cdot 1$ $\text{ClH}_2\text{C}-\text{CH}_2\text{Cl}$	$\approx -23$	45	41	4
$C_{60}\cdot 1$ $\text{Cl}_2\text{H}-\text{CCH}_2\text{Cl}$	$\approx -58$	48	46	this work

Finally, two very similar solvates ( $C_{60}\cdot 1$  DCAN and  $C_{60}\cdot 1$  TCAN) with almost identical  $C_{60}$  molecular packings surprisingly behave differently on aging. Although the natural trend of the more volatile component is to evaporate leading to the spontaneous destruction of the solvate, it is still to be understood why this process is very rapid for DCAN and so slow for TCAN.

**Acknowledgment.** This work has been supported by INTAS contract no. 93-2133 Ext, grant no. APC 1999-0143 (DGES, Spain), and the Région Centre (France, contract np. 95298060). One of us (R.C.) acknowledges an invited position from the Generalitat de Catalunya and financial support from BIOCODEX Laboratories, France (Dr. J. Vincent). The authors are grateful to Pr. X. Solans (University of Barcelona) and X. Alcobé (Serveis Científico-Tècnics, University of Barcelona) for data collections, and to P. Y. Sizaret and A. M. Carriot (Unité de Microscopie Électronique, Faculté de Médecine de Tours) for help in SEM experiments.

CM0011099